Proceedings of 20th International Congress on Acoustics, ICA 2010

23–27 August 2010, Sydney, Australia

Diffraction of bulk waves on phononic crystals

Sarah Herbison (1), Nico F. Declercq (1), Rayisa Moiseyenko (2), and Vincent Laude (2)

(1) Georgia Institute of Technology, GT-CNRS UMI 2958,
Woodruff School of Mechanical Engineering, Georgia Tech Lorraine
Metz, France
(2) Institut FEMTO-ST, CNRS UMR 6174,
Université de Franche-Comté, Besançon, France

PACS: 43.20.El, 43.35.Bf

ABSTRACT

Phononic crystals have attracted much research interest in the last decade due to their unique properties (band gaps, etc.) and potential applications in acoustic filtering and novel transducer design, among others. Many studies have examined the acoustic wave propagation that occurs inside (infinite) phononic crystals. However, in order for phononic crystals to find application in actual devices, they must be of finite size and the diffraction that may occur on the surface of the crystal becomes important. This work presents the results of experiments performed on a 2D phononic crystal consisting of steel cylinders in a water matrix. The diffraction of bulk waves that occurs on the exterior surface of the crystal will be examined, and the surface of the crystal will be shown to function as an acoustic diffraction grating. In addition, angular scans of the diffracted fields will examine the possibility of surface wave generation along the exterior surface of the crystal. It is expected that these results will contribute to a better understanding of finite-size phononic crystals and aid in the development of devices employing such crystals.

INTRODUCTION

Research interest in sonic and phononic crystals [1] has increased substantially within the last decade. These artificial crystals are inhomogeneous materials that consist of periodic arrangements of inclusions embedded within a host material, and they are the acoustical counterparts of photonic crystals in optics. Several classes of these crystals exist; for example, they may be constructed using solid inclusions within a fluid, or solid inclusions within another solid, etc. The interest in phononic crystals is due mainly to the unique properties that stem from their periodicity, such as the existence of bands of frequencies which are unable to propagate within the structure, usually referred to as band-gaps [2, 3]. Many studies have already been performed in order to determine the width and location of band-gaps in various types of phononic crystals, and the results have revealed that the contrasts in the acoustic velocities (elastic constants) and mass densities of the constituent materials of the crystal are of critical importance [4].

Potential applications for phononic crystals can be found in acoustic filtering and novel transducer designs [5, 6] as well as in the creation of vibrationless environments [7]. However, in order to bridge the gap between fundamental research of phononic crystals and the actual design of devices that may contain such crystals, a thorough understanding of effects that occur due to a crystal's finite size is required. This work presents an experimental study of the diffraction that occurs on the surfaces of a two-dimensional phononic crystal that consists of a triangular lattice arrangement of steel cylinders in water. Prior studies have observed diffraction of surface waves on finite-size phononic crystals [8], and it is expected that the surface of the crystal under study in this work may behave as a diffraction grating for bulk waves. We expect diffraction due to Bragg scattering from the cylinders, in both the incident half-space (reflected waves) and the exit half-space (transmitted waves). Within a frequency band gap, however, the transmitted waves are efficiently suppressed and we thus expect that enhanced diffraction efficiency for reflected waves could be observed.

This paper is organized in the following manner. First, the phononic crystal under study will be described, followed by an explanation of the experimental setup employed. The experimental results will then be presented, followed by conclusions.

DESCRIPTION OF THE PHONONIC CRYSTAL

The triangular lattice phononic crystal studied in this work was constructed at Institut FEMTO-ST using 575 steel cylinders, each having a diameter of 1.2 mm and a length of 150 mm. Additional studies on this crystal can be found in Ref. [9]. The cylinders were aligned using two supporting plates that had been machined to have periodic arrays of holes. The cylinders were arranged in a triangular lattice pattern as shown in Figure 1, and the distance between the centers of any two adjacent cylinders was measured to be 1.4 mm. Steel and water were chosen

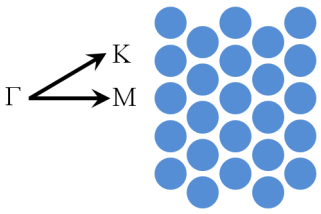

Figure 1: Diagram of the triangular lattice pattern of the crystal along with directions of highest symmetry.

as the constituent materials due to the large contrast in their densities and elastic constants. This has been shown to be an effective approach in other studies on phononic crystals [5, 10]. Theoretical band structure calculations have been performed using the Plane Wave Expansion (PWE) method. In order to

determine whether diffraction is enhanced for frequencies that lie within a band-gap, it is first necessary to determine the band-gaps of the crystal theoretically and compare these results to transmission measurements. Figure 2 shows the theoretical band structures that have been calculated for this crystal for the frequency ranges that are examined experimentally.

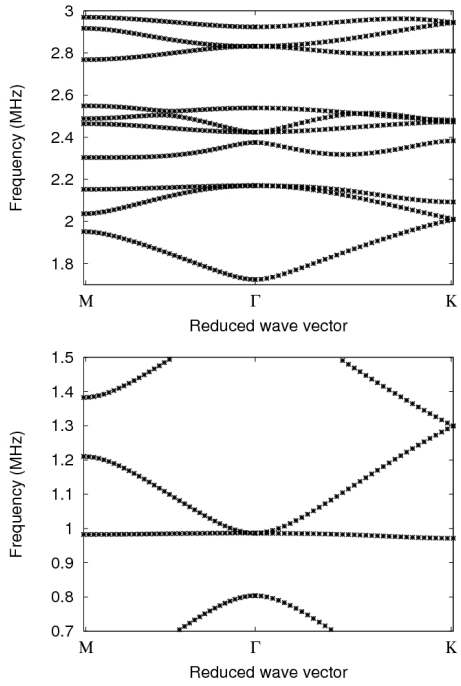

Figure 2: Theoretical band structures calculated for the two-dimensional steel-water phononic crystal.

EXPERIMENTAL SETUP

A recently developed polar/C-scan apparatus at Georgia Tech Lorraine and an ultrasonic immersion tank have been employed for all the measurements. To measure the diffracted fields generated in the incident half-space, an emitting transducer is first mounted so that it is stationary and normally incident on the crystal. The distance between the emitter and the crystal surface is approximately 74 mm. The crystal can be rotated so that the emitter can be directed along either the ΓM or the ΓK direction. A receiving transducer is mounted in a rotating fork attached to the polar/C-scan robot, and it is aimed at the point on the crystal surface where the emitter is incident. The center of rotation of the receiver is set to be even with the crystal surface.

An angular scan is performed where waveforms are collected at many angles within the diffracted field. Frequency analysis is then performed on the waveforms in order to determine the frequencies present in the field as a function of the angle. The angular range for all the diffraction measurements is 40°, from 20° to 60° with respect to the normal to the crystal surface, as shown in Figure 3.

Additional diffraction measurements designed to measure the field close to the crystal surface have an angular range of 40° to 110° with respect to the normal to the crystal surface. The experimental setup is also able to accommodate reflection measurements through the omission of the receiving transducer. A photo of the experimental setup before it was placed in the immersion tank (it is therefore shown without the receiving transducer) is shown in Figure 4.

Commercially available ultrasonic immersion transducers are

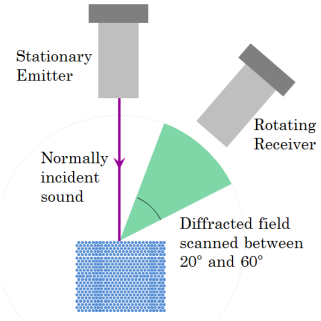

Figure 3: Schematic of experimental setup for diffraction measurement.

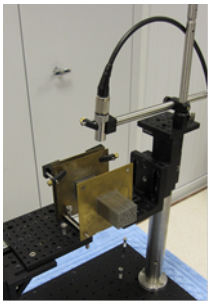

Figure 4: Experimental setup to measure diffraction on the surface of the phononic crystal.

used for all measurements. Two pairs of transducers are employed, one pair with a nominal center frequency of 1 MHz (Valpey-Fisher IS0104GP), and the other with a nominal center frequency of 2.25 MHz (Technisonics ISL-0203-SP). The beam width of all transducers employed is approximately 10 mm. The frequency spectra of the transmission between the transducer pairs are shown in Figure 5. For the diffraction measurements, the distance between the receiving transducer and the crystal surface is 45 mm for the 1 MHz transducer pair and 40.6 mm for the 2.25 MHz transducer pair.

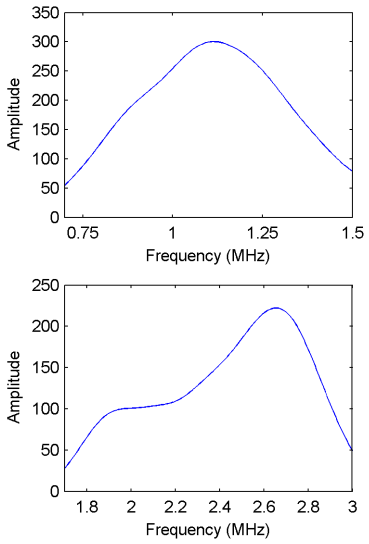

Figure 5: (Top) Frequency spectrum of transmission between 1 MHz transducer pair: 20 dB gain. (Bottom) Frequency spectrum of transmission between 2.25 MHz transducer pair: 0 dB gain.

In order to measure the transmission, the emitting transducer from the diffraction setup is removed and the rotating polar/C-scan fork is used to hold both the emitting and receiving transducers normal to the crystal surface. Due to the fixed geometry

of the rotating fork, the distance between the transducers and the crystal surface is between 25 and 30 mm, depending on the brand of transducer. Again, the crystal can be rotated to accommodate both the ΓM and ΓK directions. It should be noted that due to the geometry of the polar/C-scan robot, the diffraction measurements were taken just beyond the second crystal support plate, whereas the transmission measurements were taken for the region of the crystal between the two support plates, which was a better configuration to guarantee the periodicity of the cylinders of the crystal.

Because transmission and diffraction involving phononic crystals are extremely frequency dependent, the use of pulsed ultrasound in such experiments has limitations, namely increased noise for frequencies far from the center frequency of the pulse. In an attempt to overcome these limitations, we have also measured transmission and diffraction for this crystal using a swept frequency technique, whereby the emitter is driven by a function generator and the frequency of the sinusoidal signal changes over time.

For the 1 MHz transducer pair, a sweep from 0.5 MHz to 1.7 MHz with a duration of 1 ms was used. The frequency range of the sweep for the 2.25 MHz transducer pair was between 1.4 MHz and 4 MHz and the sweep duration was also 1 ms. Figure 6 shows the classical spectrograms (short-time FFTs) for the frequency sweeps between the 1 MHz and 2.25 MHz transducer pairs. The start and stop frequencies for the sweeping technique are beyond the range of frequencies detected in the pulsed transmission between the transducer pairs, in an effort to maximize the range of transducer response.

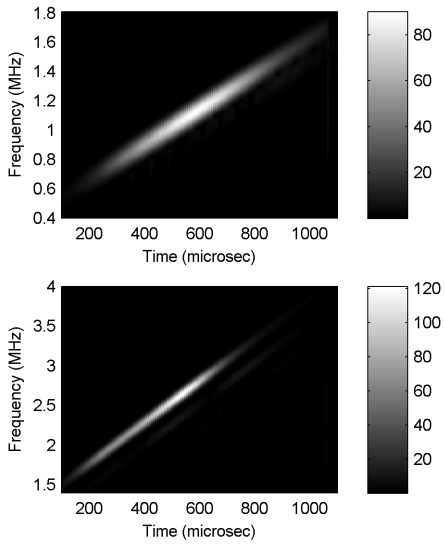

Figure 6: Classical spectrograms of transmission between transducer pairs using swept frequency technique. (Top) 1 MHz transducer pair: 20 dB gain. (Bottom) 2.25 MHz transducer pair: 0 dB gain.

EXPERIMENTAL RESULTS

Transmission Results

First, transmission measurements were performed on the crystal in order to compare with the theoretical band structure calculations. All measurements taken using pulses are obtained with 16 averages and are normalized with respect to the spectra obtained between the transducer pairs in the absence of the crystal. All data is sampled at 200 MHz. Differing gain levels are noted in the figure captions. The transmission spectra obtained from the 1 MHz transducer pair (pulsed ultrasound technique) in the ΓM and ΓK directions are shown in Figure 7. For incidence along the ΓM direction, we observe a lack of transmission for frequencies between 0.9 MHz and 1.1 MHz as well as those above 1.4 MHz. For the ΓK direction, we observe a lack of transmission for frequencies below 1.1 MHz and approximately between 1.2 MHz and 1.4 MHz.

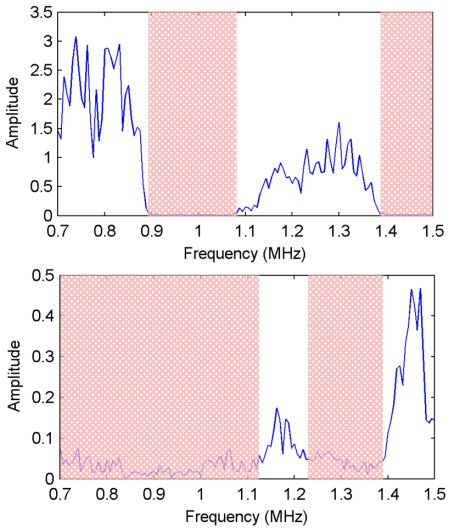

Figure 7: Transmission spectra obtained from the 1 MHz transducer pair using a pulsed ultrasound technique. 40 dB gain. (Top) ΓM direction. (Bottom) ΓK direction.

Because the ultrasound transmitted through the crystal arrives over time, a classical spectrogram (STFT) was also made of the transmitted signals in order to visualize potential band-gap regions in a different manner. The classical spectrograms obtained from the transmitted pulses between the 1 MHz transducer pair for the ΓM and ΓK directions are shown in Figure 8. Regions of reduced transmission are delimited by the dotted lines, and these regions correspond with the shaded areas in the spectra of Figure 7.

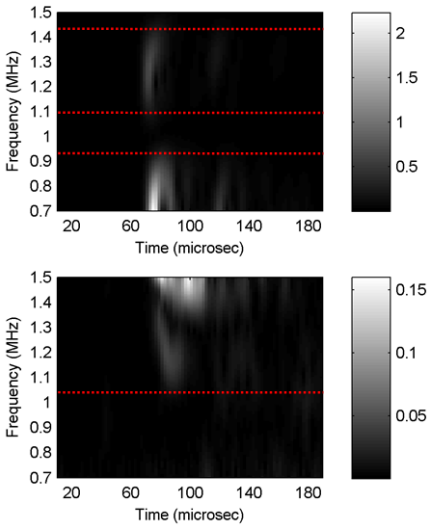

Figure 8: Classical spectrograms of transmission obtained from the 1 MHz transducer pair using a pulsed ultrasound technique. 40 dB gain. (Top) ΓM direction. (Bottom) ΓK direction.

In an effort to improve the signal-to-noise ratio for frequencies far from the center frequencies of the transducer pairs, the transmission through the crystal was also measured using a swept frequency technique. Figure 9 shows the classical spectrograms obtained for transmission through the crystal in both the ΓM

and ΓK directions using the swept frequency technique with the 1 MHz transducer pair. The classical spectrograms were created using the short-time Fourier transform (STFT) with 3000 data points for each time window. Regions of reduced transmission are delimited by the dotted lines, and these are in good agreement with the results obtained using pulsed ultrasound.

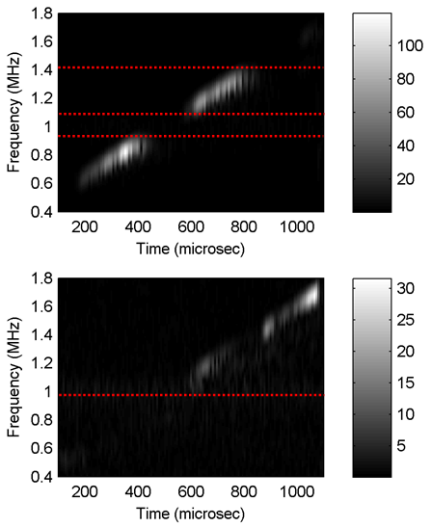

Figure 9: Classical spectrograms of transmission obtained from the 1 MHz transducer pair using a swept frequency technique. 40 dB gain. (Top) ΓM direction. (Bottom) ΓK direction.

Figures 10 and 11 show the transmission spectra obtained using pulses and the 2.25 MHz transducer pair. It should be noted that in the top spectogram of Figure 11, energy between 2.5 MHz and 2.8 MHz (circled in the figure) arrives much later than the rest of the signal. This energy was not present in the time window used to obtain the spectrum shown in the top of Figure 10, which explains its absence there. This late arrival may signal a slow group velocity or it may be an aliasing effect due to the signal processing, both possibilities meriting further investigation. The shaded rectangular areas and the dotted lines delimit regions of reduced transmission.

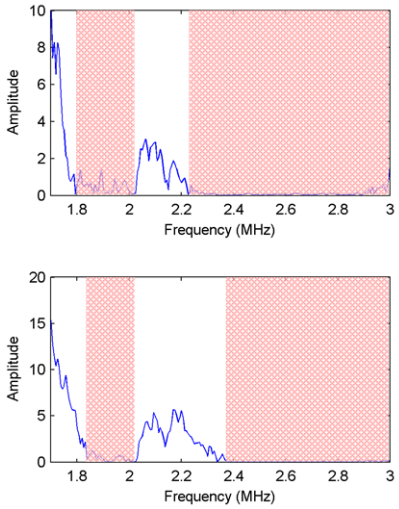

Figure 10: Transmission spectra obtained from the 2.25 MHz transducer pair using a pulsed ultrasound technique. (Top) ΓM direction. 35 dB gain. (Bottom) ΓK direction. 26 dB gain.

The classical spectrograms of Figure 12 are obtained using the 2.25 MHz transducer pair with a swept frequency technique. The regions of reduced transmission correspond well with those

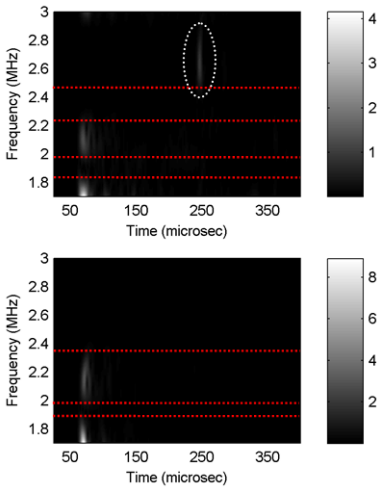

Figure 11: Classical spectrograms of transmission obtained from the 2.25 MHz transducer pair using a pulsed ultrasound technique. (Top) ΓM direction. 35 dB gain. (Bottom) ΓK direction. 26 dB gain.

found using the pulsed ultrasound, and the late arrival of energy between 2.5 MHz and 2.8 MHz for incidence in the ΓM direction is also visible in these spectrograms.

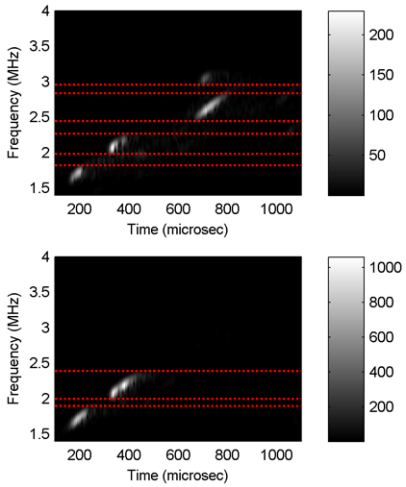

Figure 12: Classical spectrograms of transmission obtained from the 2.25 MHz transducer pair using a swept frequency technique. 40 dB gain. (Top) ΓM direction. (Bottom) ΓK direction.

Diffraction Results

The results obtained from the angular scans of the diffracted fields are now presented. The angular resolution for scans obtained using pulsed ultrasound is 0.1°, and the results are normalized with respect to the transmission spectra obtained for the transducer pairs without the presence of the crystal. For scans performed using the swept frequency technique, the angular resolution was lowered to 0.5° due to the amount of computer memory that is required for the data acquisition in this technique.

Figure 13 shows the frequencies detected as a function of angle in the diffracted field using pulsed ultrasound and the 1 MHz transducer pair. The top of the figure shows the diffraction occurring on the surface of the crystal when the incident sound is directed in the ΓM direction, and the bottom of the figure shows the result when the incident sound is directed in the ΓK

direction. In particular, we observe higher amplitude diffraction around 1 MHz for incidence in the ΓK direction which may be due to enhanced diffraction of frequencies that lie within a band-gap. The dotted lines that are superimposed on the angular spectrograms that follow are the theoretical Bragg scattering curves as explained below.

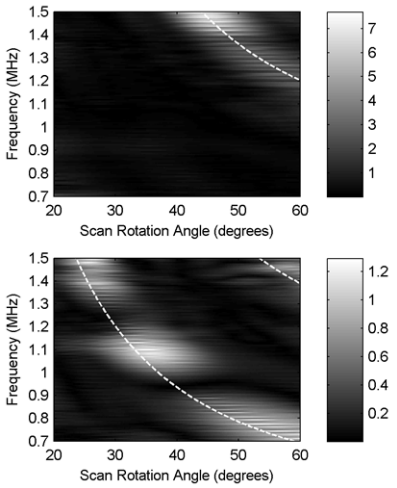

Figure 13: Angular spectrograms of diffracted frequencies obtained from the 1 MHz transducer pair using a pulsed ultrasound technique. (Top) ΓM direction. 1st order Bragg scattering visible. (Bottom) ΓK direction. 1st and 2nd order Bragg scattering visible. Theoretical Bragg scattering curves plotted with dotted lines.

The frequency and angle pairs that experience diffraction due to the periodicity of the surface of the crystal (and form theoretical Bragg scattering curves) have been calculated from Eq. (1), which can be derived from the classical diffraction grating equation [11].

$$\sin\theta_m = \frac{v_{liq} m}{f\Lambda} \tag{1}$$

The value of v_{liq} is 1459.5 m/s, which is the experimentally determined sound velocity in the water used in these experiments. The surface periodicity Λ is equal to 1.4 mm when the incident sound is directed at the surface in the ΓM direction. For the ΓK direction, the surface periodicity is no longer equal to the distance between the centers of two consecutive cylinders; it is instead equal to 2.4 mm. The variable m in Eq. (1) denotes the diffraction order, and in the experiments reported in this work, is equal to either 1 or 2. The angle θ_m is the angle at which the diffraction order m of frequency f will be diffracted into the liquid, given the surface periodicity Λ and sound velocity in the liquid v_{liq}.

The diffracted fields generated using the 2.25 MHz transducer pair were also measured. The angular spectrogram showing frequencies detected in the angular range 20° to 40° for incidence along the ΓM direction using the pulsed ultrasound is shown in Figure 14. We observe some discontinuity in the experimentally observed diffraction near 1.8 MHz and 2.4 MHz which may be related to the band-gap frequencies of the crystal.

The diffraction measurements between 20° to 40° were repeated using a swept frequency technique, and although the figures are omitted for brevity, the results appear to be very similar to those that are obtained using the pulsed ultrasound technique.

Finally, measurements were made of the diffracted field generated in the vicinity of the surface of the sample using pulsed ultrasound from the 2.25 MHz transducer pair incident in the

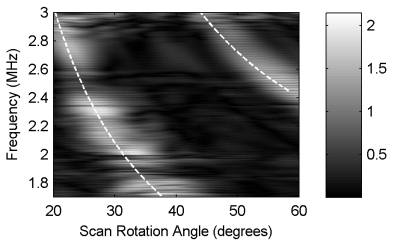

Figure 14: Angular spectrogram of diffracted frequencies obtained from the 2.25 MHz transducer pair using pulsed ultrasound technique with incidence along the ΓM direction. 10 dB gain. 1st and 2nd order Bragg scattering visible and theoretical Bragg scattering curves plotted with dotted lines.

ΓM direction. The resulting angular spectrogram is shown in Figure 15. The theoretical 2nd order Bragg scattering curve is seen to follow the experimentally detected diffracted frequency and angle pairs. Further investigation of phenomena that may be occurring on the surface of the crystal (90° rotation angle) should be conducted.

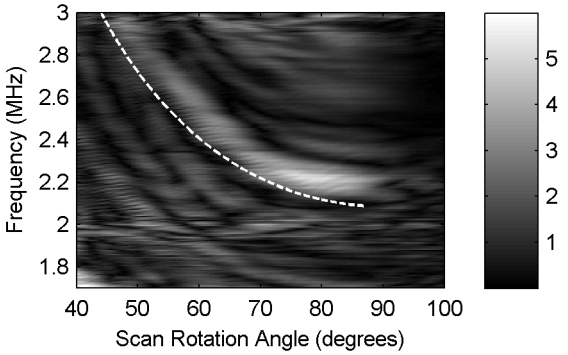

Figure 15: Angular spectrogram of diffracted frequencies obtained from the 2.25 MHz transducer pair with pulsed ultrasound incident along the ΓM direction. 26 dB gain. Theoretical 2nd order Bragg scattering plotted with dotted line.

Because the theoretical Bragg scattering curves closely follow the experimentally detected diffracted frequencies in the angular spectrograms generated from measurements of the diffracted field in the incident half-space, it can be said that the surface of the crystal is functioning as an acoustic diffraction grating, which has implications for devices that may employ bulk acoustic waves in combination with finite-size phononic crystals.

CONCLUSIONS

This work has examined the use of pulsed and swept-frequency ultrasound in order to investigate the transmission and diffraction that occurs on a finite-size two-dimensional phononic crystal consisting of steel cylinders in water. The diffraction that is observed to occur on the surface in the incident half-space is followed closely by the theoretical Bragg scattering curves. The surface of the phononic crystal is therefore observed to function as an acoustic diffraction grating. Some discontinuities and regions of higher amplitude of the diffraction are observed, which may be due to the location of these frequencies with respect to the band-gaps for the crystal. This has implications in the design of devices that may incorporate finite-size phononic crystals along with bulk acoustic waves.

ACKNOWLEDGEMENTS

The authors would like to acknowledge the French *Centre National de Recherche Scientifique* (CNRS) and the *Conseil Ré-*

gional de Lorraine for their financial support of this work. Financial support by the *Agence Nationale de la Recherche* under grant ANR-09-BLAN-0167-01 is gratefully acknowledged.

REFERENCES

[1] J. H. Page et al. "Phononic Crystals". *Phys. Status Solidi B* 241 (2004), pp. 3454–3462.

[2] J.V. Sánchez-Pérez et al. "Sound Attenuation by a Two-Dimensional Array of Rigid Cylinders". *Phys. Rev. Lett.* 80 (1998), pp. 5325–5328.

[3] Vincent Laude et al. "Full band gap for surface acoustic waves in a piezoelectric phononic crystal". *Phys. Rev. E* 71 (2005), p. 036607.

[4] J.O. Vasseur et al. "Experimental evidence for the existence of absolute acoustic band gaps in two-dimensional periodic composite media". *J. Phys.: Condens. Matter* 10 (1998), pp. 6051–6064.

[5] A. Khelif et al. "Guiding and bending of acoustic waves in highly confined phononic crystal waveguides". *Appl. Phys. Lett.* 84 (2004), pp. 4400–4402.

[6] C. Goffaux et al. "Measurements and calculations of the sound attenuation by a phononic band gap structure suitable for an insulating partition application". *Appl. Phys. Lett.* 83 (2003), pp. 281–283.

[7] M.S. Kushwaha and P. Halevi. "Band gap engineering in periodic elastic composites". *Appl. Phys. Lett.* 64 (1994), pp. 1085–1087.

[8] Kimmo Kokkonen et al. "Scattering of surface acoustic waves by a phononic crystal revealed by heterodyne interferometry". *Appl. Phys. Lett.* 91 (2007), p. 083517.

[9] Fu-Li Hsiao et al. "Complete band gaps and deaf bands of triangular and honeycomb water-steel phononic crystals". *J. Appl. Phys.* 101 (2007), p. 044903.

[10] A. Khelif et al. "Trapping and guiding of acoustic waves by defect modes in a full-band-gap ultrasonic crystal". *Phys. Rev. B* 68 (2003), p. 214301.

[11] Erwin G. Loewen and Evgeny Popov. *Diffraction Gratings and Applications*. New York: Marcel-Dekker, 1997.